

# Experimental Evaluation of Interactive Edge/Cloud Virtual Reality Gaming over Wi-Fi using Unity Render Streaming

Miguel Casanovas\*, Costas Michaelides, Marc Carrascosa-Zamacois, Boris Bellalta

*Wireless Networking Research Group, Universitat Pompeu Fabra  
Carrer de Roc Boronat 138, 08018 Barcelona, Spain*

---

## Abstract

Virtual Reality (VR) streaming enables end-users to seamlessly immerse themselves in interactive virtual environments using even low-end devices. However, the quality of the VR experience heavily relies on Wi-Fi performance, since it serves as the last hop in the network chain. Our study delves into the intricate interplay between Wi-Fi and VR traffic, drawing upon empirical data and leveraging a simulator tailored to VR traffic patterns. In this work we further evaluate Wi-Fi's suitability for VR streaming in terms of the quality of service it provides. In particular, we employ Unity Render Streaming to remotely stream real-time VR gaming content over Wi-Fi 6 using WebRTC, leveraging a server physically located at the network's edge, near the end user. Our findings demonstrate the system's sustained network performance, showcasing minimal round-trip time and jitter at 60 and 90 fps. In particular, we uncover the characteristics and patterns of the generated traffic streams, unveiling a surprising video transmission approach inherent to WebRTC-based services. This approach involves the fragmentation of video frames into discrete batches of packets, transmitted at regular intervals regardless of the targeted frame rate. This segmentation mechanism maintains consistent video packet delays across video frame rates but leads to increased Wi-Fi airtime consumption at higher frame rates. The presented results demonstrate that shortening the interval between batches is advantageous as it improves Wi-Fi efficiency and reduces delays in delivering complete frames.

*Keywords:* Virtual Reality, Wi-Fi, Cloud Gaming, Edge Computing, Unity, WebRTC

---

## 1. Introduction

Virtual Reality (VR) has received significant attention for its transformative potential across multiple sectors, including multimedia, entertainment, gaming, healthcare, and education [1]. Notably, the VR market is expected to witness significant growth, with an anticipated annual increase of 27.5% from 2023 to 2030 [2]. However, VR demands substantial computational power, particularly relying on high-performance Graphics Processing Units (GPUs) and Central Processing Units (CPUs) to achieve optimal rendering of graphics and maintain low-latency interactions for seamless, immersive gaming experiences.

In response to the computational demands of VR, remote rendering has emerged as a pivotal solution. By offloading resource-intensive rendering tasks to dedicated servers, it effectively alleviates the burden on local devices. Thereby, this approach not only enhances accessibility to sophisticated, high-quality VR games but also fosters the

scalability of VR, accommodating a broader range of devices.

Remote rendering leverages distinct distributed computing paradigms, including cloud computing and edge computing. Cloud computing relies on remote, centralized data centers for ubiquitous, on-demand access to shared resources. Hence, Cloud VR services such as PlutoSphere<sup>1</sup> and XRStream<sup>2</sup>—both powered by Nvidia CloudXR<sup>3</sup>—deliver VR experiences over the internet without requiring sophisticated local hardware. Nevertheless, the inherent distance between users and cloud servers can lead to significant latency concerns. In contrast, edge computing brings the computational resources to the network's edge, close to the end user. Thus, Edge VR minimizes latency and enhances real-time responsiveness, optimizing the delivery of immersive VR experiences.

Despite the benefits of remote rendering, delivering VR content over a network poses significant challenges, stemming primarily from the stringent bandwidth and latency requirements inherent to immersive VR experiences. Indeed, motion-to-photon latency should remain beneath 15

---

\*Corresponding author

*Email addresses:* miguel.casanovas@upf.edu (Miguel Casanovas), costas.michaelides@upf.edu (Costas Michaelides), marc.carrascosa@upf.edu (Marc Carrascosa-Zamacois), boris.bellalta@upf.edu (Boris Bellalta)

---

<sup>1</sup><https://www.plutosphere.com/>

<sup>2</sup><https://xrstream.co/>

<sup>3</sup><https://developer.nvidia.com/cloudxr-sdk/>

ms to prevent motion sickness [3, 4]. Notably, ultimate VR is anticipated to demand substantial bandwidth, exceeding 1 Gbps, to achieve an unparalleled level of immersion [5–7]. In our previous research [8], we empirically evaluated Edge VR streaming performance over Wi-Fi 6 (IEEE 802.11ax) to multiple users using Air Light VR (ALVR)<sup>4</sup>, specifically in terms of latency. Our results demonstrated seamless VR streaming to three standalone Head-Mounted Displays (HMDs) at up to 100 Mbps per user, using either the Distributed Coordination Function (DCF) or DCF plus Orthogonal Frequency Division Multiple Access (OFDMA) only in the downlink (DL). Notably, uplink (UL) OFDMA scheduling disrupted the timely delivery of tracking data. In this work, we leverage Unity’s Render Streaming plugin<sup>5</sup> to deliver remotely rendered Edge VR gaming content over Wi-Fi 6 using WebRTC<sup>6</sup>. Our study delves into the characteristics of VR traffic, unveiling the presence of multiple periodic data streams with distinct generation patterns in both the DL and UL directions. Additionally, our work encompasses an experimental assessment of the system’s performance, underscoring its ability to deliver VR content, particularly at high frame rates. We investigate Wi-Fi’s shaping effects on packet temporal arrangement, highlighting Access Point (AP) video packet aggregation and congestion-related delays. Our video traffic analysis yields a significant finding: video frames (VFs) are fragmented into batches of packets that are transmitted every 5.56 ms. Each batch may correspond to a segment of a VF based on a slice encoding approach. Notably, delivering a VF in time-spaced batches sustains similar DL packet delays but prolongs the delivery of complete frames. Additionally, it leads to higher Wi-Fi channel occupancy as higher frame rates are used.

Consequently, this work contributes to the field of VR streaming by:

1. Showcasing Unity’s Render Streaming capability for delivering VR games to end-users using Wi-Fi. Indeed, VR Quality of Service (QoS) requirements are easily met under normal operating conditions, achieving low latency with Round-Trip Time (RTT) consistently below 5 ms, minimal jitter, and no packet loss at 60 and 90 frames per second (fps).
2. Enhancing our understanding of WebRTC-based VR systems’ traffic patterns, with an emphasis on the fragmentation of VFs in temporally spaced batches of packets and its impact on streaming performance metrics such as packet delay and VF assembly delays.
3. Highlighting the interplay between Wi-Fi’s and Unity’s remotely rendered VR traffic. In particular, we provide insights on the relationship between

streaming parameters—such as video frame rate and inter-batch time—and Wi-Fi’s packet aggregation capabilities. Additionally, we delve into their collective influence on spectrum resource utilization.

The paper is structured as follows: Section 2 offers a comprehensive overview of the foundational elements of this work. Section 3 overviews the related work. Section 4 outlines our research methodology, including the experimental design. Sections 5 to 8 encompass the experimental evaluation. Section 5 details the traffic structure and data streams. Section 6 delves deeper into the video stream. Section 7 thoroughly assesses streaming performance. Section 8 explores Wi-Fi’s and Unity’s VR traffic interplay. Finally, Section 9 concludes this work.

## 2. WebRTC, Unity Render Streaming and Wi-Fi

### 2.1. WebRTC

WebRTC is an open-source project standardized by the World Wide Web Consortium (W3C)<sup>7</sup> and the Internet Engineering Task Force (IETF)<sup>8</sup>. This technology enables secure peer-to-peer (P2P) communication, providing real-time communication (RTC) capabilities via application programming interfaces (APIs) [9].

WebRTC implementations incorporate congestion control mechanisms to enhance RTC efficiency. For instance, the Google Congestion Control algorithm [10], implemented in commercial browsers such as Google Chrome, dynamically adjusts the transmission rate based on network conditions, using a delay-based controller at the receiver and a loss-based controller at the sender.

WebRTC relies on standardized protocols, including:

- Interactive Connectivity Establishment (ICE) [11]: ICE is used to determine the optimal communication path. It uses STUN and TURN for Network Address Translation (NAT) traversal.
- Session Traversal Utilities for NAT (STUN) [12]: STUN is used to discover the public IP address and port of an endpoint located behind a NAT. Additionally, it is used to assess connectivity and serves as a keep-alive mechanism to maintain NAT bindings.
- Traversal Using Relays around NAT (TURN) [13]: TURN is used to relay data when direct P2P communication is hindered by network constraints.
- Session Description Protocol (SDP) [14]: SDP is used to exchange media capabilities and session details.
- Secure Real-Time Protocol (SRTP) [15]: SRTP ensures the secure transport of real-time media, providing confidentiality, integrity, and authentication.

<sup>4</sup><https://github.com/alvr-org/ALVR/>

<sup>5</sup><https://github.com/Unity-Technologies/UnityRenderStreaming/>

<sup>6</sup><https://webrtc.org/>

<sup>7</sup><https://www.w3.org/>

<sup>8</sup><https://www.ietf.org/>

- Secure Real-Time Control Protocol (SRTCP) [15]: SRTCP securely delivers control and statistical information related to the Real-Time Protocol (RTP) [16, 17] media stream.
- Datagram Transport Layer Security (DTLS) [18, 19]: DTLS provides security for datagram-based communications through integrated key management and parameter negotiation.

## 2.2. Unity Render Streaming

Unity<sup>9</sup> is a versatile cross-platform game engine designed for creating interactive 2D and 3D experiences. Unity uses C# as its primary programming language and integrates drag-and-drop functionalities. Additionally, it provides built-in features and developer tools specifically tailored for building immersive Extended Reality (XR)<sup>10</sup> experiences, including support for the OpenXR<sup>11</sup> standard.

Unity’s Render Streaming plugin enables remote real-time rendering and streaming of interactive experiences to the web using WebRTC. This open-source solution offloads resource-intensive rendering processes from the client’s device to a dedicated rendering server running Unity.

Signaling is handled by a *node.js* web server, enabling direct P2P communication via User Datagram Protocol (UDP) [20]. The rendering server integrates Unity’s WebRTC package<sup>12</sup>, while the client relies on WebRTC’s native JavaScript APIs within the web browser. Nevertheless, both peers leverage common interfaces, including *RTCPeerConnection* to establish and manage the P2P connection and *RTCDataChannel* for reliable bidirectional communication of non-media data.

Unity Render Streaming enables the configuration of video codec, target frame rate (default up to 60 fps), bitrate (default up to 10 Mbps), and resolution. Additionally, it offers support for several input methods within the web browser, including mouse, keyboard, touch, and gamepad. Notably, it does not currently offer support for VR specific systems as remote input sources. Nevertheless, it can be seamlessly integrated with WebXR<sup>13</sup> to capture the input from VR devices, as demonstrated in [21, 22].

The remote streaming process using Unity’s Render Streaming plugin unfolds as follows: the client captures user interactions within the web browser and sends them to the server. The server processes the incoming data, updates the game state, and generates the corresponding visual content. The rendered content is encoded into a video stream and transmitted to the client. Upon reception, the client decodes and displays the visual content in the user’s web browser (see Fig. 1).

## 2.3. Wi-Fi 6 - IEEE 802.11ax

Wi-Fi 6 (IEEE 802.11ax) is an amendment to the IEEE 802.11 Physical (PHY) and Medium Access Control (MAC) layers to enhance operational efficiency [24–26].

Wi-Fi 6 operates on 2.4 and 5 GHz frequency bands, supporting channel bandwidths up to 160 MHz. Wi-Fi 6E extends this standard into the 6 GHz spectrum. The fundamental channel access scheme of Wi-Fi 6 is the Distributed Coordination Function (DCF). DCF relies on Carrier Sense Multiple Access with Collision Avoidance (CSMA/CA) to manage access to the communication medium. The basic units of data transmission are MAC Protocol Data Units (MPDUs). However, multiple MPDUs can be aggregated into a single Aggregated MPDU (A-MPDU) to enhance data transmission efficiency by reducing overhead. This process is commonly referred to as *packet aggregation*. Moreover, Wi-Fi 6 introduces Orthogonal Frequency Division Multiple Access (OFDMA) for frequency multiplexing (F-MUX). OFDMA divides the available frequency spectrum into multiple orthogonal sub-channels, called Resource Units (RUs), enabling multiple users to access the network simultaneously. Wi-Fi 6 also integrates both Single User (SU) and Multi-User (MU) Multiple Input Multiple Output (MIMO) for spatial multiplexing (S-MUX), incorporating MU-MIMO in the UL. MIMO enables the simultaneous transmission and reception of multiple data streams by using multiple antennas.

This standard offers substantial improvements in data rates, network capacity, and efficiency compared to its predecessor, Wi-Fi 5 (IEEE 802.11ac)—please refer to Table 1 for a comparative overview. Hence, Wi-Fi 6 stands out as a compelling candidate for providing the essential connectivity required to enable real-time, wireless VR gaming experiences.

Table 1: Wi-Fi 5 and Wi-Fi 6 features comparison. Adapted from [27].

	Wi-Fi 5	Wi-Fi 6
<b>Frequency</b>	5 GHz	2.4, 5, 6 GHz
<b>Bandwidth (MHz)</b>	20,40,80,80+80,160	20,40,80,80+80,160
<b>MCS</b>	up to 256-QAM	up to 1024-QAM
<b>Data Rate</b>	up to 7 Gbps	up to 9.6 Gbps
<b>TWT</b>	No	Yes
<b>BSS Coloring</b>	No	Yes
<b>F-MUX</b>	OFDM	OFDM, DL/UL OFDMA
<b>S-MUX</b>	SU-MIMO, DL MU-MIMO	SU-MIMO, DL/UL MU-MIMO

## 3. Related work

In the landscape of remote gaming, Cloud Gaming (CG) has garnered significant research attention, leading to studies on its protocols and traffic dynamics. For instance, Di Domenico et al. [28] identified distinct protocol implementations in several CG services. Notably, Google Sta-

<sup>9</sup><https://unity.com/>

<sup>10</sup>Extended Reality encompasses Virtual Reality (VR), Augmented Reality (AR), and Mixed Reality (MR)

<sup>11</sup><https://www.khronos.org/openxr/>

<sup>12</sup><https://github.com/Unity-Technologies/com.unity.webrtc/>

<sup>13</sup><https://immersiveweb.dev/>

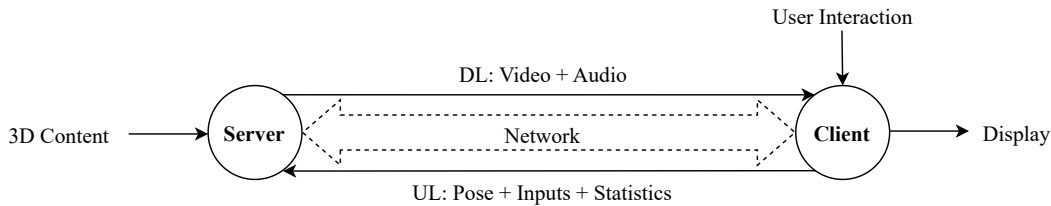


Figure 1: Remote streaming process. Adapted from [23].

dia<sup>14</sup> leveraged WebRTC, GeForce NOW<sup>15</sup> relied on RTP for multimedia streaming without standardized session establishment protocols, and PlayStation Now<sup>16</sup> adopted a proprietary UDP-based approach. Moreover, multiple studies have modeled the traffic generated by CG platforms using client-side gathered data [29, 30]. Manzano et al. [29] meticulously examined the OnLive<sup>17</sup> CG platform traffic, unveiling the characteristics of multiple RTP streams. In particular, the RTP video flow exhibited regular VF bursts, split into multiple packets. Interestingly, video packets demonstrated inter-arrival times up to 6 ms. Carrascosa et al. [30] conducted an extensive assessment of Google Stadia’s traffic, uncovering traffic generation patterns within the downstream RTP stream: a consistent 1/fps inter-frame interval and  $\approx 2$  ms interval video batches within each frame period.

Nevertheless, research on cloud-driven VR is scarce. Notably, Zhao et al. [31] investigated VR CG under fixed and adaptive bitrate encoding schemes, using Paperspace<sup>18</sup>, a commercial CG service provider, and Virtual Desktop<sup>19</sup>. The authors highlighted the advantages of adaptive bitrate, including reduced latency and frame loss. Additionally, their traffic analysis disclosed two successive sequences of video packets within each VF, providing distinct perspectives for each eye.

In contrast, several works have replicated Cloud VR schemes within controlled, local environments using edge computing servers. For instance, Li et al. [32] evaluated ALVR’s performance, highlighting the substantial impact of limited bandwidth and high packet loss on frame rate and latency. Surprisingly, VR gamers barely perceived RTT values up to 90 ms. Vikberg’s experimental research [33] focused on optimizing and evaluating WebRTC for Cloud VR using Unity Render Streaming. The author analyzed diverse configurations to minimize latency, pinpointing resolution reduction and rendering rate increase as effective strategies. Lee et al. [34] leveraged Unity’s WebRTC-based remote streaming solution, showing that an increase in concurrent users reduced each user’s data

rate and led to increased jitter and dropped frames. On the other hand, Korneev et al. [35] analyzed stereoscopic RTP VR traffic using the Pico Streaming Assistant<sup>20</sup>. The authors highlighted single-slice VF encoding and bimodal frame size distribution.

Similarly, numerous studies have leveraged servers close to end-users for wireless VR streaming over Wi-Fi. Salehi et al. [36] explored edge-enabled VR traffic using ALVR, uncovering VFs are generated every 1/fps and fragmented into multiple MPDUs. Their findings indicated that increasing bitrates does not consistently enhance quality across applications and results in larger VFs that may impose additional strain on the network. Building upon their work in [37], Chiariotti et al. [38] conducted a fundamental VR traffic characterization using RiftCat. 2.0<sup>21</sup>. The authors unveiled the underlying traffic streams and highlighted the occurrence of frame rate aligned VF bursts. Interestingly, the packets comprising a VF were transmitted collectively within a single batch. Alhilal et al. [39] examined the impact of concurrent users on network data transfer rates within social WebRTC-based VR platforms such as Mozilla Hubs<sup>22</sup>. The authors observed that an increase in the number of concurrent users led to a substantial rise in startup delay. Jansen et al. [40] assessed the network performance and requirements for wireless VR offloading to the edge using Android Debug Bridge<sup>23</sup>. Their findings underscored the need for a stable, high-throughput network. Interestingly, despite lower resource utilization, Edge VR led to increased battery depletion compared to native processing.

Thus, research on VR streaming has predominantly revolved around performance [32–34, 40] and traffic characteristics [31, 35–39], using diverse hardware such as standalone HMDs [31–33, 36, 39, 40], smartphones [33, 37, 38], and computers [34]. Notably, several studies have further contributed to the field by presenting VR traffic models [35, 37, 38].

To the best of our knowledge, this is the first work in the literature that delves into the intricacies of Unity’s WebRTC-based VR traffic and unveils the segmentation of VFs into temporally spaced batches of packets. Indeed,

<sup>14</sup>Shutdown in January 2023, <https://stadia.google.com/gg/>

<sup>15</sup><https://play.geforcenow.com/>

<sup>16</sup>Recently integrated to PlayStation Plus, <https://www.playstation.com/en-us/ps-plus/>

<sup>17</sup>Shutdown in April 2015

<sup>18</sup><https://www.paperspace.com/>

<sup>19</sup><https://www.vrdesktop.net/>

<sup>20</sup><https://www.picoxr.com/global/software/pico-link/>

<sup>21</sup><https://riftcat.com/vridge/>

<sup>22</sup><https://github.com/mozilla/hubs/>

<sup>23</sup><https://developer.android.com/studio/command-line/adb/>

prior studies in CG and VR remote rendering highlighted distinct RTP video traffic dynamics [30, 31, 35, 37, 38]. Our study not only demonstrates the system’s ability to meet VR QoS requirements but also delves into the influence of video batching on streaming performance, Wi-Fi’s packet aggregation, and spectrum efficiency.

#### 4. Methodology

In this section, we provide a detailed description of the experimental environment and the data collection and analysis procedures.

##### 4.1. Experimental setup

The experiments were conducted within a controlled, server-based local environment comprising a server, an AP, and a client (see Fig. 2 and Fig. 3).

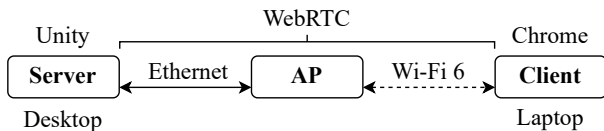


Figure 2: Testbed components.

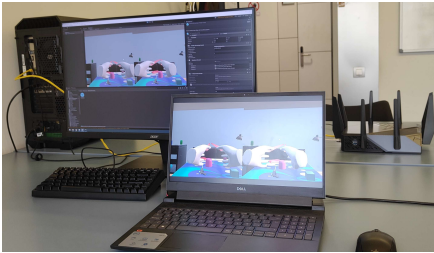


Figure 3: A snapshot of the experimental setup.

The testbed was established at the UPF’s Department of Information and Communication Technologies (DTIC) in Barcelona, Catalonia, Spain. The gaming-centric AP is Wi-Fi 6 (IEEE 802.11ax) compliant and works at the 5 GHz band using a 80 MHz channel. The server, a high-performance gaming desktop, was connected to the AP via Ethernet, ensuring a stable and reliable connection. The client, a VR-Ready laptop, sustained a robust Wi-Fi 6 connection with an RSSI of -46 dBm, leveraging 2 spatial streams (SS) for enhanced data transmission. The favorable network conditions enabled the utilization of the highest achievable modulation and coding scheme (MCS): 1024-QAM and a 5/6 coding rate. The client device enabled the capture of network traffic on the client side and integrated keyboard and mouse input methods, seamlessly supported by Unity’s Render Streaming. Equipment specifications are detailed in Table 2.

The server, running Unity (v2021.3.6f1), rendered and streamed the VR games content to the client over WebRTC using Unity Render Streaming. It also served as the signaling server through a WebSocket connection. The

Table 2: Experimental equipment.

<b>Desktop</b>	CPU	i5-12600KF
	SSD	500GB NVMe
	GPU	NVIDIA® GeForce RTX™ 3080, 10 GB
	NIC	Realtek Gaming 2.5GbE
	RAM	32GB DDR5 4800 MHz
	OS	Windows 10 x64
<b>AP</b>	Model	ASUS ROG Rapture GT-AX11000
	FW	3.0.0.4.388_22525
<b>Laptop</b>	Model	Dell G15 5521 Special Edition
	CPU	i7-12700H
	GPU	NVIDIA® GeForce RTX™ 3060 Laptop
	WNIC	Intel® Killer™ Wi-Fi 6 AX1650i 2x2
	OS	Windows 11 x64

client accessed the web-based application using the Google Chrome browser (v113.0.5672.93) and decoded and displayed the rendered content while capturing user inputs. Pulover’s Macro Creator<sup>24</sup> (v5.4.1) facilitated the recording and playback of predefined mouse and keyboard inputs at the client, ensuring a systematic and reproducible testing environment. This method enabled continuous adjustment of the viewpoint’s rotation, reproducing the sensitivity of VR HMDs in tracking subtle changes in head orientation. Consequently, as outlined in Appendix A, the video generated using either a laptop or an HMD as input sources remained consistent in characteristics.

The foundation of our investigation relied on *Alteration Hunting* (AH)<sup>25</sup>, an immersive VR experience we developed using Unity v2021.3.6f1. In addition, we conducted a comparison of AH’s traffic characteristics with two open-source sample scenes: the *XR Interaction Toolkit 2.3* (ITK)<sup>26</sup> demo scene and *The Escape Room* (ER)<sup>27</sup> VR experience from Unity Learn. Each game was customized to integrate Unity’s remote streaming solution, including Unity’s Render Streaming plugin (v3.1.0-exp.4) and Unity’s WebRTC package (v3.0.0-pre.1). Unity’s Render Streaming plugin was extended to support up to 90 fps and 100 Mbps, surpassing the 60 fps and 10 Mbps constraints outlined in Section 2.2. Specifically, the adjustments involved modifying range constraints in the *VideoStreamSender.cs* script, as illustrated in the code snippet below.

```

public class VideoStreamSender : StreamSenderBase
{
    // Previous code

    // [SerializeField, FrameRate] // Original
    [SerializeField] // Updated

    // [SerializeField, Bitrate(0, 10000)] // Original
    [SerializeField, Bitrate(0, 100000)] // Updated (kbps)

    // Rest of the class implementation
}
  
```

<sup>24</sup><https://www.macrocreator.com/>

<sup>25</sup><https://github.com/miguelcupf/AlterationHunting/>

<sup>26</sup><https://github.com/Unity-Technologies/XR-Interaction-Toolkit-Examples/>

<sup>27</sup><https://assetstore.unity.com/packages/templates/tutorials/vr-beginner-the-escape-room-163264/>

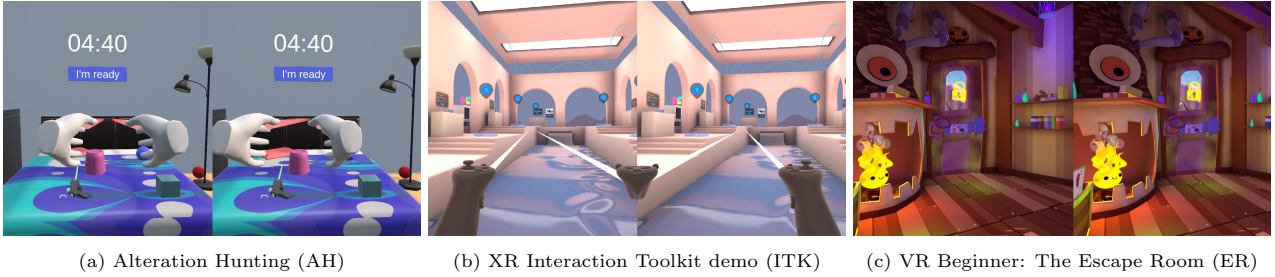


Figure 4: Screenshots of the VR games.

Furthermore, the VR games were upgraded to present a stereoscopic view by placing left and right eye cameras with a 63 mm interpupillary distance, ensuring that each camera spans half of the viewport horizontally (see Fig. 4).

Notably, the NVENC<sup>28</sup> hardware-accelerated encoder was used to encode video in the H.264 Constrained Baseline 5.1 format. Additional video streaming configurations encompassed the target frame rate, bitrate, and resolution. A 90 fps frame rate ensured a smooth gaming experience and aligned with the screen refresh rates of multiple VR devices. Incorporating 60 and 30 fps enabled the evaluation of frame rate impact on system performance and traffic dynamics. A constant bitrate (CBR) of 50 Mbps ensured the attainment of consistent and reliable results in our Edge VR setup where bandwidth fluctuations were minimal. The video streaming resolution, set at 3664x1920p (1832x1920p per eye), adhered to the specifications of several HMDs, including the Oculus Quest 2.

#### 4.2. Data collection and analysis

Data collection encompassed multiple one-minute trials, including three for AH at each target frame rate (30, 60, and 90 fps) and one each for ITK and ER at 90 fps. Wireshark (v4.0.5)<sup>29</sup> was used for capturing network traffic from both endpoints. The collected traffic traces were processed using *tshark* to extract relevant UDP data, including *frame.time\_relative*, *frame.len*, *\_ws.col.Protocol*, and *\_ws.col.Info*, into a CSV file. WebRTC statistics [41], encompassing encoded and decoded fps<sup>30</sup>, RTT<sup>31</sup>, jitter<sup>32</sup>, and packet loss<sup>33</sup>, were also gathered from the client and server. Server statistics were extracted in JSON format using Unity’s WebRTC package, whereas client statistics were stored in TXT format via `chrome://webrtc-internals`. Hence, each dataset<sup>34</sup> includes *tshark*-processed traffic traces and WebRTC statistics from both the client and server

Data analysis, leveraging the Python programming language and the Pandas library,<sup>35</sup> focused on a 30-second window of active gameplay.

## 5. Traffic characteristics

In this section, our focus is on analyzing the traffic structure and identifying the data streams involved in the transmission process. The analysis relies on traces collected from the server side for DL traffic and from the client side for UL traffic, providing insights into traffic generation in both directions. It encompasses Alteration Hunting, the XR Interaction Toolkit demo, and Escape Room at 90 fps.

### 5.1. Overview

Fig. 5 displays the empirical cumulative distribution function (ECDF) of the the inter-packet time for both DL and UL directions, showing consistency among the analyzed games. Remarkably, the DL consistently exhibits shorter time intervals between packets, indicating a higher packet transfer rate. Indeed, over 95.8% of the data packets are transmitted in the DL, underscoring a significant disparity in packet distribution.

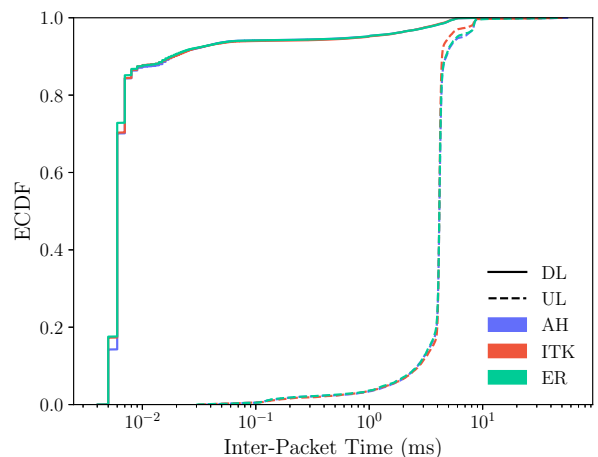


Figure 5: Inter-packet time ECDF for different games at 90 fps.

<sup>28</sup><https://developer.nvidia.com/video-codec-sdk/>

<sup>29</sup><https://www.wireshark.org/>

<sup>30</sup>*framesEncoded* field from *RTCOutboundRtpStreamStats* and *framesDecoded* field from *RTCInboundRtpStreamStats*

<sup>31</sup>*roundTripTime* field from *RTCRemoteInboundRtpStreamStats*

<sup>32</sup>*jitter* field from *RTCReceivedRtpStreamStats*

<sup>33</sup>*packetsLost* field from *RTCReceivedRtpStreamStats*

<sup>34</sup>The datasets are publicly available on Zenodo [42]

<sup>35</sup><https://pandas.pydata.org/>



## 5.2. Traffic streams

Several WebRTC data streams, leveraging UDP as the underlying transport protocol, have been observed, each serving distinct purposes:

- STUN messages are exchanged to check connectivity between endpoints.
- The SRTP stream securely transports real-time audio and video data, distinguishable by payload type or Synchronization Source Identifier (SSRC).
- The SRTCP stream carries control information, providing feedback on the transmitted data quality.
- The DTLS stream is responsible for delivering arbitrary data through the data channel, including input and pose data in the UL.
- Generic UDP packets are potentially related to network synchronization or timing.

Table 3 provides a comprehensive overview of the characteristics of each generated stream. Notably, the DL constitutes  $\approx 99.3\%$  of the traffic load. The SRTP video stream accounts for the largest volume of data in the DL ( $\approx 99.5\%$ ), while DTLS packets are the primary traffic in the UL ( $\approx 85.0\%$ ).

The different traffic streams exhibit similar traffic characteristics across distinct games. However, the Escape Room’s SRTP Audio stream displays a significantly higher load due to the presence of an active background audio source, distinguishing it from the other games that only include sound effects when certain actions are played. Additionally, UL generic UDP packets, which are deemed insignificant with respect to the total traffic, show variations in packet timing between the three games.

Therefore, building upon the shared characteristics observed across games, the rest of the paper relies on Alteration Hunting as a representative sample.

## 5.3. Temporal patterns

The SRTP Video stream exhibits periodic bursts of data, surprisingly surpassing the anticipated intervals according to the 90 fps target frame rate (see Fig. 6). Given this unexpected phenomenon, and the fact that the video stream constitutes more than 98% of the traffic, we devote Section 6 to studying its behavior and characteristics.

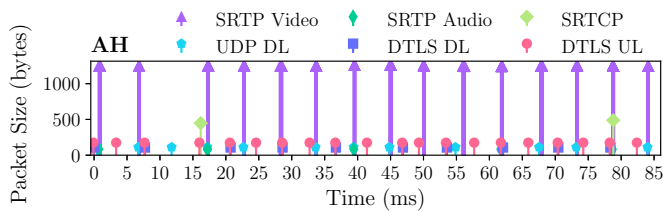


Figure 6: Traffic streams temporal evolution at 90 fps.

The remaining streams demonstrate discernible temporal patterns (see Fig. 7):

- STUN traffic displays the recurring exchange of binding requests and 106-byte responses. DL requests and their responses occur every  $\approx 2.5$  s, while UL requests and their responses happen every  $\approx 2.65$  s.
- The SRTP Audio traffic generation pattern discerns the systematic arrangement of packets into alternating batch types, even in the absence of an active audio source. These batches comprise 8 and 7 arrival instances, spanning  $\approx 140$  ms and  $\approx 120$  ms, respectively, with a  $\approx 30$  ms gap between successive batches.
- SRTCP packets are transmitted at regular  $\approx 62.5$  ms intervals, regardless of the frame rate.
- UL DTLS packets are generated at the client’s display refresh rate (240 Hz, every  $\approx 4.16$  ms), while DL DTLS packets occur at half the frequency (120 Hz, every  $\approx 8.33$  ms).
- Generic UDP packets exhibit a bimodal distribution of inter-packet times in the DL (every  $\approx 5.56$  ms and  $\approx 11.1$  ms), while no discernible pattern is observed in the UL.

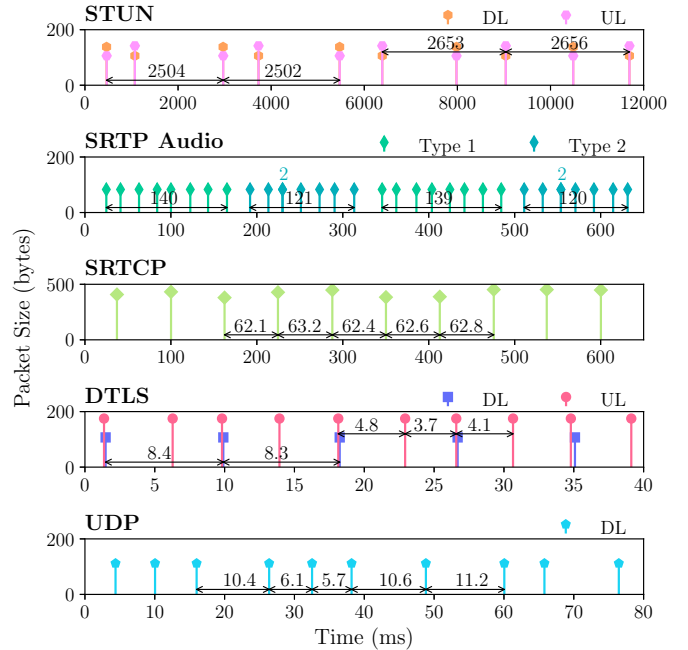


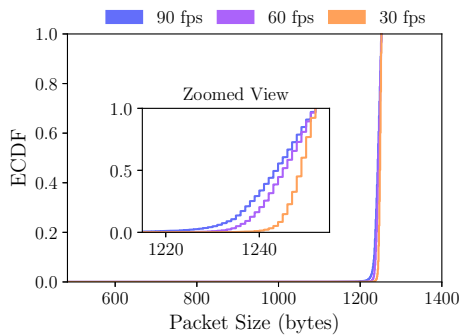
Figure 7: Traffic pattern of each stream.

## 6. Video traffic

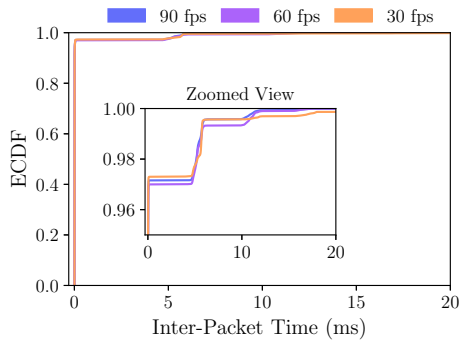
This section studies the video stream traffic, placing the focus on the occurrence of video traffic batches that surpass the targeted frame rate. The analysis encompasses Alteration Hunting traces at several target frame rates, including 90, 60, and 30 fps.

Table 3: Traffic streams characteristics for different games at 90 fps: mean packet size (Bytes), mean inter-packet time (ms), and load (Mbps).

	AH			ITK			ER		
	Bytes	ms	Mbps	Bytes	ms	Mbps	Bytes	ms	Mbps
<b>Downlink</b>									
STUN	122	1287.42	0.0008	122	1288.10	0.0008	122	1288.45	0.0008
SRTP Audio	83	20	0.033	83	20.01	0.033	730.90	20.01	0.29
SRTP Video	1242.16	0.19	53.45	1242.61	0.19	53.63	1243.56	0.19	53.38
DTLS	107.01	8.94	0.096	107.01	8.74	0.098	107.01	8.89	0.096
Generic UDP	112	8.26	0.11	112	8.24	0.11	112.16	8.23	0.11
<b>Uplink</b>									
STUN	124	1287.48	0.0008	124	1288.21	0.0008	124	1288.50	0.0008
SRTCP	434.62	67.27	0.052	421.68	63.97	0.053	418.92	63.56	0.053
DTLS	174.97	4.90	0.31	174.96	4.38	0.32	174.96	4.46	0.32
Generic UDP	147.64	443.75	0.0026	143.31	576.86	0.0020	138.96	639.26	0.0017

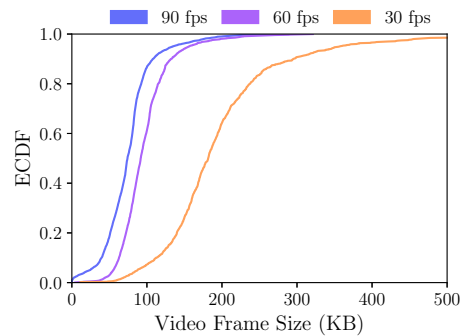


(a)

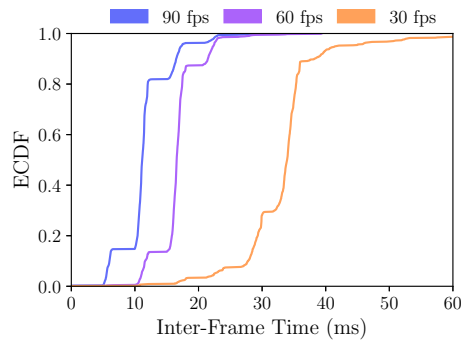


(b)

Figure 8: Video packet size and inter-packet time ECDFs.



(a)



(b)

Figure 9: VF size and inter-frame time ECDFs.

### 6.1. Characteristics of video packets

The SRTP Video stream exhibits consistent packet characteristics across games (see Table 3). Notably, as depicted in Fig. 8a, video packet sizes strongly skew towards the 1220 to 1252 Bytes range. On the other hand, Fig. 8b illustrates that a substantial portion of packets ( $\approx 97\%$ ) exhibit microsecond-level inter-packet times, while the remaining packets manifest intervals in the order of milliseconds, forming discernible batches.

### 6.2. Characteristics of video frames

Video content is transmitted as sequences of VFs with variable sizes. Intuitively, as depicted in Fig. 9a, the distribution of similar data volumes (i.e., the bitrate is fixed

to 50 Mbps regardless the fps transmitted) over a higher number of fps leads to lower video frame sizes. Conversely, Fig. 9b illustrates the ECDF of the time lapse between consecutive VFs. Consistent with our expectations, the inter-frame period is closely correlated with the frame rate, averaging around  $1/\text{fps}$ : 33.33 ms at 30 fps, 16.67 ms at 60 fps, and 11.11 ms at 90 fps.

### 6.3. Video batching

In our analysis of traffic traces, we observed that VFs are systematically partitioned into batches transmitted at discrete intervals, regardless of the frame rate (see Fig. 10). In particular, batch transmission points occur every  $\approx 5.56$  ms. Nevertheless, idle instances arise when a complete



frame is dispatched before the initiation of the subsequent frame’s transmission.

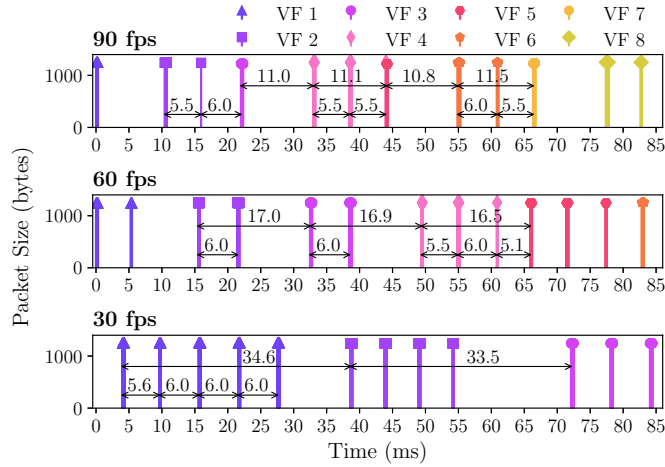


Figure 10: Video stream temporal evolution for Alteration Hunting at different fps.

Fig. 11 delves into the distribution of video data within individual transfer instances occurring every 5.56 ms, showcasing variability in the packet count. The histogram reveals that around 15% of the transmission instances exhibit no packets at 90 fps. In contrast, idle instances rise to 20% and 25% at 60 fps and 30 fps, respectively. Thus, despite lower frame rates exhibiting heightened segmentation due to larger VFs, prolonged inter-frame periods result in additional transmission points for each frame, leading to more idle transfer intervals.

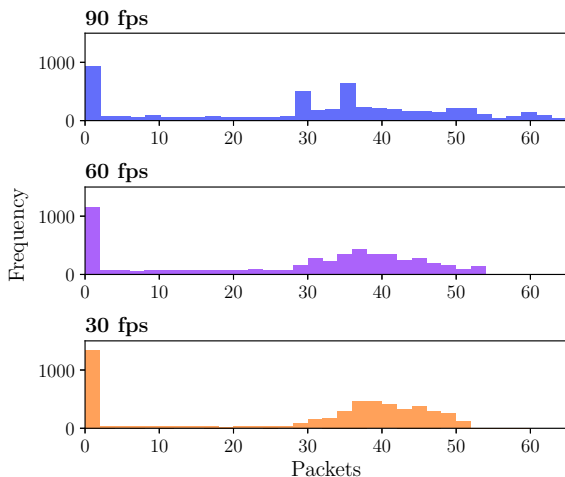


Figure 11: Histogram of video packets sent every 5.56 ms.

Our hypothesis posits that each batch of packets corresponds to a segment of a VF, adhering to slice-based encoding principles. Given the use of H.264 encoding, our conjecture is that each batch constitutes a single Network Abstraction Layer Unit (NALU). NALUs serve as fundamental units of H.264-encoded video data. Each NALU is

sequentially encoded, fragmented into several RTP packets at the application layer—rather than relying on the network’s Maximum Transmission Unit (MTU) [43]—and delivered to the network.

## 7. Streaming performance

In this section, we shift our focus towards validating the streaming performance and QoS attainment, leveraging WebRTC statistics gathered from both ends during the streaming of Alteration Hunting.

### 7.1. Decoded fps

The number of frames decoded per second provides valuable insights into the stability and consistency of the streaming system.

Notably, Fig. 12 confirms our system’s reliable operation up to 90 fps, given that encoded frames are successfully decoded and the target frame rate is nearly attained. Interestingly, at 90 fps, Unity Render Streaming appears to approach its operational threshold as the encoder struggles to maintain a consistent video frame rate.

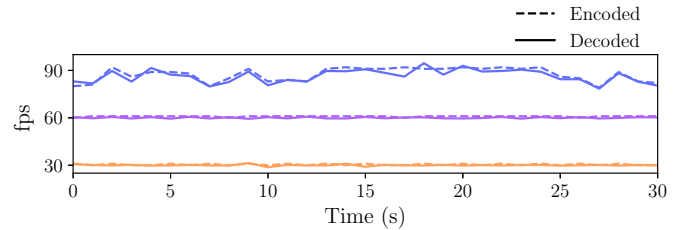


Figure 12: Encoded and decoded fps temporal evolution.

### 7.2. Key performance indicators

RTT, jitter, and packet loss are crucial indicators of network performance and key factors for assessing QoS in WebRTC-based services [44]. According to the International Telecommunication Union Telecommunication Standardization Sector (ITU-T), VR services require RTT values below 20 ms, jitter levels under 15 ms, and a packet loss rate beneath 0.001% [45, 46].

Interestingly, Fig. 13a displays uniform RTT performance across frame rates, averaging 1.5 ms. Notably, the reported RTT values, estimated based on RTCP timestamps, align with ITU-T recommendations, contributing to motion sickness prevention. Fig. 13b shows that higher frame rates lead to reduced video jitter delay. Specifically, per-packet video jitter values revolve around 20 ms for 30 fps, 9 ms for 60 fps, and 7 ms for 90 fps, consistently adhering to ITU-T guidelines for 60 fps and 90 fps. This increase in jitter at lower frame rates may stem from larger VF sizes and heightened idle batch transfer instances, contributing to a less evenly spaced delivery of packets.

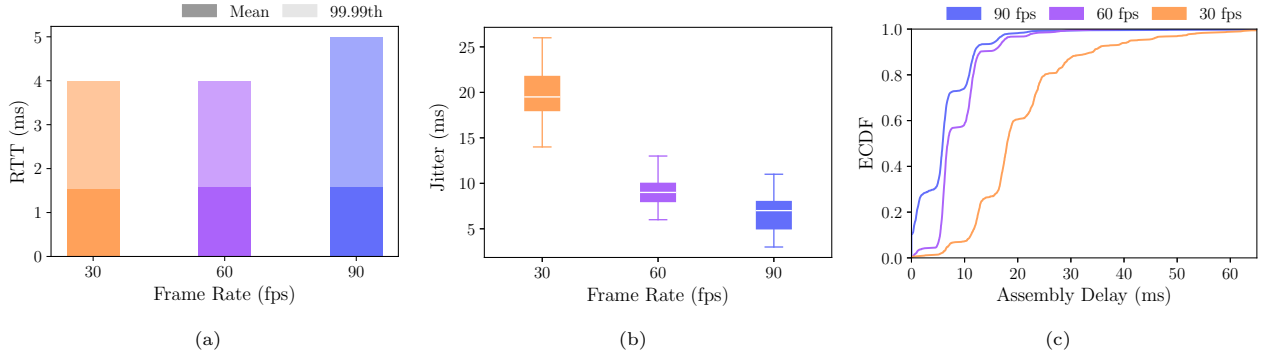


Figure 13: Streaming performance metrics at different fps.

The absence of lost packets, regardless of the targeted frame rate, indicates sustained network performance. Hence, the VR streaming system attains the QoS goals at target frame rates of 60 and 90 fps.

### 7.3. Assembly delay

Assembly delay refers to the time elapsed between the reception of the first and last RTP packet within a VF. Hence, minimizing this temporal gap is paramount for the timely delivery of seamless and responsive experiences.

Interestingly, as illustrated in Fig. 13c, lower frame rates exhibit larger assembly delays. Specifically, assembly delays average around 21 ms at 30 fps, 9 ms at 60 fps, and 6 ms at 90 fps. This is a result of splitting VFs into batches transmitted every 5.56 ms, as larger frame sizes lead to heightened frame segmentation. Hence, this fragmentation mechanism inherently leads to longer assembly delays than simultaneously delivering a VF in a single batch.

## 8. Wi-Fi and VR traffic interplay

In the previous sections, we delved into the intricacies of the generated traffic and validated the streaming performance. Nevertheless, the wireless network infrastructure can significantly disrupt VR traffic patterns, potentially compromising the quality of experience. In addition, the effects of delivering fragmented VFs in temporally spaced batches require closer scrutiny. Hence, this section delves into the interplay between Wi-Fi networks and Unity’s WebRTC-based VR traffic, relying on both empirical data and simulations.

### 8.1. Wi-Fi’s impact on VR traffic: real-world tests

To assess the network’s impact on VR traffic dynamics, we first leverage Alteration Hunting traffic traces at 90 fps from both endpoints. Fig. 14 shows that the network significantly disrupts the timing of both DL and UL packets, showcasing the occurrence of simultaneous packet arrivals. In particular, 89.7% of the DL packets and 10.1% of the UL packets are received simultaneously.

This phenomenon stems from the accumulation of packets in the AP and station transmission buffers during

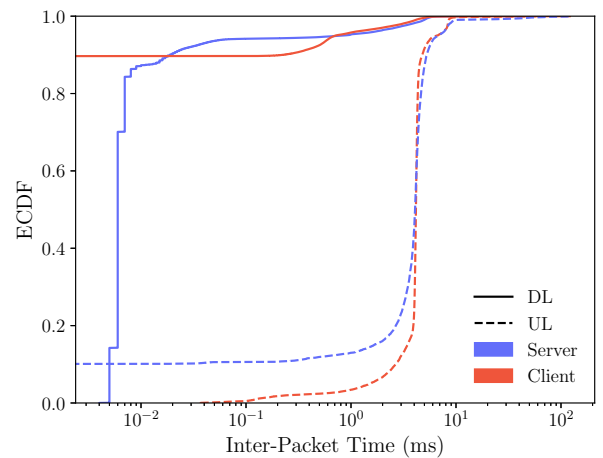


Figure 14: Inter-packet time ECDF of both DL and UL traffic.

channel access attempts, causing their aggregation into A-MPDUs, as depicted in Fig. 15 for DL video packets. Interestingly, A-MPDUs occasionally include packets from distinct VFs.

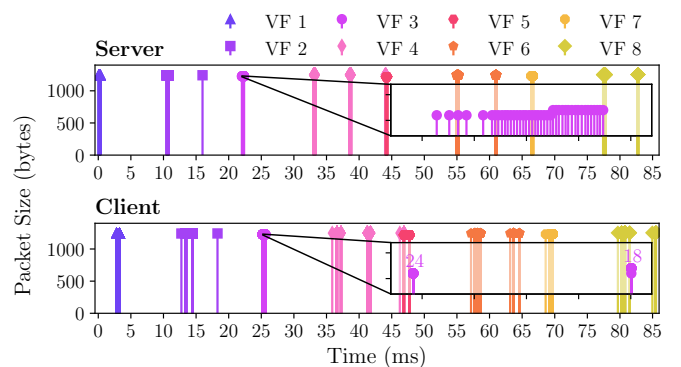


Figure 15: Video packet aggregation at 90 fps.

Using client-side DL Alteration Hunting traces at 30, 60, and 90 fps, Fig. 16 unveils consistent mean video A-MPDU sizes across frame rates, suggesting a stable data aggregation mechanism. Low video frame rates should offer more opportunities for transmitting larger A-MPDUs,

as VFs are larger in size, thus achieving a more efficient use of spectrum resources. However, it only happens occasionally, as evidenced by the 99.99th percentile in Fig. 16. Indeed, the segmentation of VFs in multiple temporally spaced batches prevents the use of large A-MPDU transmissions, leading to a nearly uniform mean A-MPDU size across frame rates.

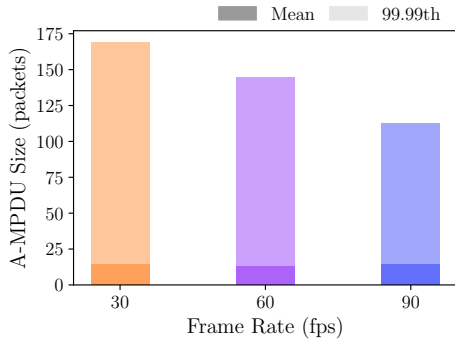


Figure 16: Video A-MPDU size for different fps: real-world tests.

## 8.2. Wi-Fi’s response to VR traffic: simulations

The preceding subsection has shown the impact of Wi-Fi random channel access and packet aggregation on the delivery of VR video packets from the AP to the client. However, comprehensively analyzing the intricate relationship between Wi-Fi and VR traffic based solely on network-layer traffic traces proves challenging.

In this section, we turn to simulations to examine how the division of VFs into multiple temporally spaced batches affects Wi-Fi’s response, particularly in terms of latency and spectrum utilization. We leverage a Wi-Fi simulator that implements the 802.11ax channel, PHY, and MAC layers, using the same settings adopted during our tests—namely, an 80 MHz bandwidth channel, 2 SS, and MCS 11, as described in Section 4.1. The simulator incorporates an interactive application model that generates both VR video traffic in the DL and control messages in the UL, matching the characteristics observed in real traces. This entails reproducing the segmentation of VF data into batches transmitted at  $\tau$  ms intervals (e.g.,  $\tau = 5.56$  ms). For each VF, the number of batches into which it will be divided is determined uniformly at random. Subsequently, the generated packets are distributed among them. Notably, to be consistent with our real-world tests, a 50 Mbps CBR is considered.

Before proceeding, let us establish a benchmark to understand the DL packet delays obtained in this section. Considering MCS 11, 2 SS, and an 80 MHz channel, a single video packet of 1243 Bytes requires 0.374 ms, including RTS/CTS, 3 SIFS, and DIFS delays. This value represents the minimum achievable latency.

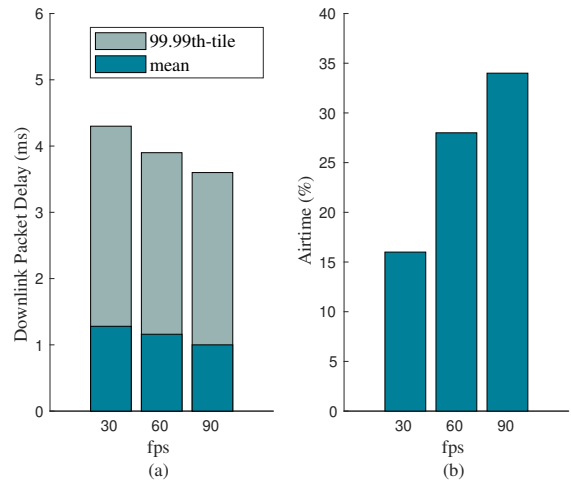


Figure 17: Downlink video packet delay and airtime.

### 8.2.1. Matching Unity’s 5.56 ms video batching

In this section, we study the case when  $\tau = 5.56$  ms, matching Unity’s traffic generation, as described in Section 6. Note that by considering frame rates of 30, 60, and 90 fps,  $\tau = 5.56$  ms allows for a maximum of 6, 3, and 2 intervals for segmenting a VF before the subsequent one, respectively.

Fig. 17a presents the DL delay in our simulations, displaying both mean and 99.99th percentile values. DL video packet delay slightly decreases as the fps increases, averaging 1.28 ms at 30 fps and 1.01 ms at 90 fps. This subtle reduction in video packet delay may seem counter-intuitive, given that the airtime required to deliver all VR traffic rises from 16% at 30 fps to 35% at 90 fps (see Fig. 17b), meaning that twice as many ‘spectrum resources’ are required to transmit the same amount of traffic. Nevertheless, the previous results can be rationalized by the fact that the bitrate remains constant.

Under a CBR video streaming scenario, an increase in frame rate leads to smaller VFs and shorter intervals between VF transmissions, leading to reduced buffer occupancy for incoming packets (see Fig. 18a). Reduced buffer occupancy contributes to a lower DL packet delay, as DL packet delay encompasses the entire time span a packet spends in the AP’s transmission buffer, which depends on the number of packets present upon its arrival. However, lower buffer occupancy implies that Wi-Fi aggregates fewer packets in each A-MPDU (see Fig. 18b). Hence, given that shorter A-MPDU transmissions are less efficient in terms of overhead reduction, more airtime is required to transmit the same volume of data.

These results unveil the impact of fragmenting VFs into batches of packets transmitted at 5.56 ms intervals. This approach reduces the amount of data delivered to the network at every transfer instance, thus further minimizing the DL packet delay. Notably, implementing this mechanism for every nominal frame rate maintains a nearly

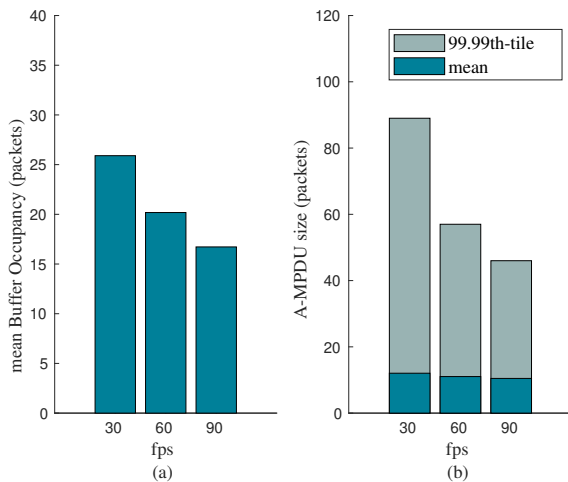


Figure 18: Buffer occupancy at packet arrivals and A-MPDU size for different fps.

constant DL packet delay, although it comes at the cost of increased spectrum resource usage as Wi-Fi transmission becomes less efficient.

### 8.2.2. Using distinct inter-batch times

In this section, we investigate the influence of distinct inter-batch times ( $\tau$ ) on DL video packet delays and VF delays to better understand the effects of delivering VFs partitioned in multiple batches. VF delay refers to the time elapsed from the moment a VF is sent to the network interface at the server until it is completely received at the client, equivalent to the assembly delay.

Fig. 19 shows the DL video packet delay and the VF delay for several inter-batch times at 60 fps. As it can be observed in Fig. 19a, neither for the mean or the 99th percentile increasing the inter-batch time has any significant effect beyond slightly reducing the mean packet delay. However, as depicted in Fig. 19b, longer inter-batch time lead to prolonged VF delays. Thus, opting for a shorter inter-batch time is clearly the optimal choice from the Wi-Fi perspective. Notably, the obtained mean VF delay using a 5.56 ms inter-batch time is consistent with the mean assembly delay in real-world tests at 60 fps (see Section 7.3).

## 9. Conclusions

In this work, we empirically assessed Wi-Fi’s suitability for delivering cloud-based VR gaming experiences, leveraging Unity. Overall, the system demonstrated sustained network performance and streaming quality at 60 and 90 fps. Nevertheless, AP bundling of video packets and network congestion intervals led to disruptions in traffic patterns.

In our in-depth traffic analysis, we discerned the existence of multiple periodic data streams, including UL

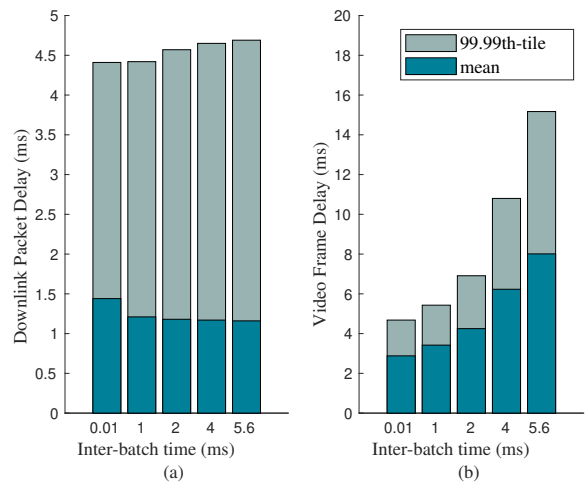


Figure 19: Downlink video packet delay and video frame delay at 60 fps.

tracking/input packets aligned with the client’s display refresh rate. Additionally, we identified frame rate aligned VF bursts within the RTP video stream. Notably, we unveiled the streaming system’s segmentation of VFs into batches of RTP packets sent every ‘5.56 ms’, a pattern not unique to Unity Render Streaming but rather prevalent in WebRTC applications, as evidenced in Appendix B. This mechanism introduces delay in the delivery of complete frames, potentially leading to increased latency and reduced responsiveness—critical aspects in real-time experiences. Additionally, while it allows to maintain a relatively consistent packet delay regardless of the targeted frame rate, it leads to increased Wi-Fi’s airtime utilization at higher frame rates, given the aggregation of fewer packets per transmission.

This paper serves as a reference for future research in interactive VR CG over Wi-Fi, building upon insights from edge-based VR streaming. In future research, our aim is to determine Unity’s optimal video encoding settings for delivering immersive VR experiences over Wi-Fi. Moreover, we plan to evaluate the system’s scalability and its performance under diverse network conditions, including network throttling and fluctuations in bandwidth and latency. Indeed, the integration of a network emulator into our Edge VR setup will allow us to mimic Cloud VR streaming conditions, providing insights into the system’s responses in realistic and dynamic network environments before reaching the last hop, i.e., the Wi-Fi connection. Additionally, we intend to explore the intricate interplay between adaptive bitrate, WebRTC congestion mechanisms, and Wi-Fi features within the realm of VR CG. Lastly, we anticipate investigating advanced Wi-Fi features and multiplayer VR streaming to understand how Wi-Fi manages the concurrent transmission of both throughput and latency-sensitive data streams.

## 10. Acknowledgments

This work is partially funded by Wi-XR PID2021-123995NB-I00 (MCIU/AEI/FEDER,UE), MAX-R EU-HE2022 (101070072), and by MCIN/AEI under the Maria de Maeztu Units of Excellence Programme (CEX2021-001195-M).

## Appendix A. VR traffic using a Meta Quest 2 HMD as the input source

Is our video traffic characterization and streaming performance evaluation representative of scenarios involving HMDs?

As described in Section 2.2, Unity Render Streaming does not feature sending VR input messages from the web client to Unity nor mapping these remote inputs to Unity actions. In order to enable genuine VR input, we leveraged a Meta Quest 2 HMD and Meta Quest Link—a feature that enables connecting a Meta Quest VR headset to a computer using a compatible USB-C cable, providing VR access to applications launched directly in Unity’s Editor<sup>36</sup>. Thus, an HMD served as the local input source, allowing us to broadcast realistic VR gameplay rendered on Unity from the server (desktop) to the client (laptop) via Unity Render Streaming (see Fig. A.20).

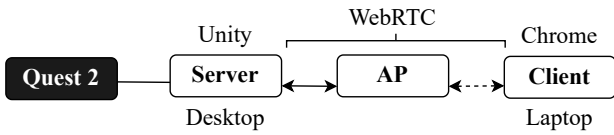


Figure A.20: Testbed components using an HMD as the input source.

Notably, using Alteration Hunting and a 90 fps target frame rate, our analysis validates the system’s performance when inputs are sourced from an HMD. In particular, no packet loss occur during transmission, and the RTT and video jitter average 1.8 ms and 7.3 ms, respectively—meeting VR services’ QoS requirements. Additionally, the generated video stream remains consistent whether inputs originate from an HMD or a laptop. Indeed, the only significant traffic disparity lies in the encoded frame rate, as Unity synchronizes with the HMD’s default 72 Hz display refresh rate (see Fig. A.21).

## Appendix B. Video batching in other WebRTC-based applications

In Section 6.3, we unveiled Unity’s Render Streaming plugin systematic partitioning of VFs into several batches of RTP packets transmitted every 5.56 ms. This prompts a fundamental inquiry: Is the observed behavior caused by

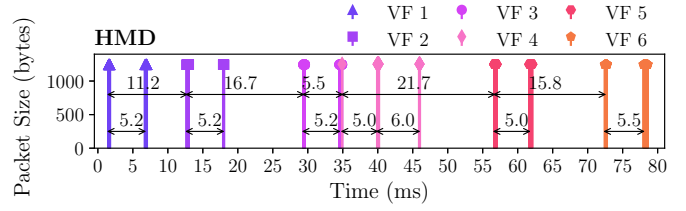


Figure A.21: Video stream temporal evolution using Meta Quest Link and Alteration Hunting at 90 fps.

Unity’s plugin? To ascertain this, this section is devoted to investigating the traffic patterns of other WebRTC-based services, including GeForce NOW and Google Meet<sup>37</sup>.

As depicted in Fig. B.22, GeForce NOW displays an inter-frame time averaging 16.68 ms, aligning with its free membership frame rate of 60 fps. On the other hand, Google Meet inter-frame time averages 33.43 ms, aligning with the broadcaster’s 1280x720@30fps camera. Interestingly, this figure underscores a prevalent pattern in WebRTC-based services, albeit with distinctions. In particular, in GeForce NOW, VFs are fragmented into batches received at  $\approx 1.4$  ms intervals. Similarly, in Google Meet, VFs are divided into multiple batches that are received at intervals averaging 5.12 ms, consistent with Unity’s Render Streaming behavior. Considering Google Meet’s use of the VP8 codec, our hypothesis is that each batch corresponds to partitions—independently encoded segments of VFs—subsequently fragmented into multiple RTP packets [47]. Hence, the fragmentation of VFs into temporally spaced batches emerges as a consistent pattern in WebRTC-based services, each adopting a distinct approach. Indeed, in [30], Google Stadia’s RTP stream also exhibited batches of video packets received every  $\approx 2$  ms within each frame period.

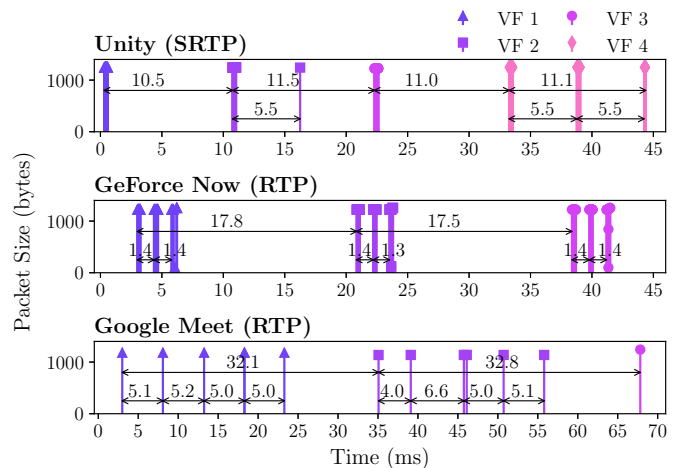


Figure B.22: Video stream temporal evolution for several WebRTC-based services.

<sup>36</sup><https://developer.oculus.com/documentation/unity/unity-link/>

<sup>37</sup><https://meet.google.com/>

## References

- [1] S. Idris, M. K. Ahmed, et al., Study and analysis of virtual reality and its impact on the current era, in: 2020 Seventh International Conference on Information Technology Trends (ITT), IEEE, 2020, pp. 20–25.
- [2] Grand View Research, Inc., Virtual Reality (VR) Market Size, Share & Trends Analysis Report, 2030, <https://www.grandviewresearch.com/industry-analysis/virtual-reality-vr-market>, [Accessed: January 30, 2024].
- [3] M. S. Elbamby, C. Perfecto, M. Bennis, K. Doppler, Toward low-latency and ultra-reliable virtual reality, *IEEE Network* 32 (2) (2018) 78–84.
- [4] F. Alriksson, C. Phillips, J. L. Pradas, A. Zaidi, et al., XR and 5G: Extended reality at scale with time-critical communication, *Ericsson technology review* 2021 (8) (2021) 2–13.
- [5] S. Mangiante, G. Klas, A. Navon, Z. GuanHua, J. Ran, M. D. Silva, Vr is on the edge: How to deliver 360 videos in mobile networks, in: Proceedings of the Workshop on Virtual Reality and Augmented Reality Network, 2017, pp. 30–35.
- [6] Huawei, Cloud vr network solution white paper, [https://www.huawei.com/minisite/pdf/ilab/cloud\\_vr\\_network\\_solution\\_white\\_paper\\_en.pdf](https://www.huawei.com/minisite/pdf/ilab/cloud_vr_network_solution_white_paper_en.pdf), [Accessed: January 30, 2024] (2018).
- [7] E. Bastug, M. Bennis, M. Médard, M. Debbah, Toward interconnected virtual reality: Opportunities, challenges, and enablers, *IEEE Communications Magazine* 55 (6) (2017) 110–117.
- [8] C. Michaelides, M. Casasnovas, D. Marchitelli, B. Bellalta, Is Wi-Fi 6 Ready for Virtual Reality Mayhem? A Case Study Using One AP and Three HMDs (2023).
- [9] World Wide Web Consortium W3C, WebRTC: Real-time Communication in Browsers, <https://www.w3.org/TR/webrtc/>, [Accessed: January 30, 2024] (March 2023).
- [10] G. Carlucci, L. De Cicco, S. Holmer, S. Mascolo, Analysis and design of the google congestion control for web real-time communication (WebRTC), in: Proceedings of the 7th International Conference on Multimedia Systems, 2016, pp. 1–12.
- [11] RFC 8445, Interactive Connectivity Establishment (ICE): A Protocol for Network Address Translator (NAT) Traversal, <https://datatracker.ietf.org/doc/html/rfc8445>, [Accessed: January 30, 2024] (July 2018).
- [12] RFC 8489, Session Traversal Utilities for NAT (STUN), <https://datatracker.ietf.org/doc/html/rfc8489>, [Accessed: January 30, 2024] (February 2020).
- [13] RFC 8656, Traversal Using Relays around NAT (TURN): Relay Extensions to Session Traversal Utilities for NAT (STUN), <https://datatracker.ietf.org/doc/html/rfc8656>, [Accessed: January 30, 2024] (February 2020).
- [14] RFC 8866, SDP: Session Description Protocol, <https://datatracker.ietf.org/doc/html/rfc8866>, [Accessed: January 30, 2024] (January 2021).
- [15] RFC 3711, The Secure Real-time Transport Protocol (SRTP), <https://datatracker.ietf.org/doc/html/rfc3711>, [Accessed: January 30, 2024] (March 2004).
- [16] RFC 8834, Media Transport and Use of RTP in WebRTC, <https://datatracker.ietf.org/doc/html/rfc8834>, [Accessed: January 30, 2024] (January 2021).
- [17] RFC 3550, RTP: A Transport Protocol for Real-Time Applications, <https://datatracker.ietf.org/doc/html/rfc3550>, [Accessed: January 30, 2024] (July 2003).
- [18] RFC 6347, Datagram Transport Layer Security Version 1.2, <https://datatracker.ietf.org/doc/html/rfc6347>, [Accessed: January 30, 2024] (January 2012).
- [19] RFC 5764, Datagram Transport Layer Security (DTLS) Extension to Establish Keys for the Secure Real-time Transport Protocol (SRTP), <https://datatracker.ietf.org/doc/html/rfc5764>, [Accessed: January 30, 2024] (May 2010).
- [20] RFC 768, User Datagram Protocol, <https://datatracker.ietf.org/doc/html/rfc768>, [Accessed: January 30, 2024] (August 1980).
- [21] R. Seligmann, et al., Web-based Client for Remote Rendered Virtual Reality (2020).
- [22] V. Mohan, GitHub - FusedVR/VR Streaming: Unity Render Streaming SDK to stream VR from CloudXR to WebXR over WebRTC, <https://github.com/FusedVR/VRStreaming>, [Accessed January 30, 2024].
- [23] S. Shi, C.-H. Hsu, A survey of interactive remote rendering systems, *ACM Computing Surveys (CSUR)* 47 (4) (2015) 1–29.
- [24] IEEE Standard for Information Technology–Telecommunications and Information Exchange between Systems Local and Metropolitan Area Networks–Specific Requirements Part 11: Wireless LAN Medium Access Control (MAC) and Physical Layer (PHY) Specifications Amendment 1: Enhancements for High-Efficiency WLAN, *IEEE Std 802.11ax-2021 (Amendment to IEEE Std 802.11-2020)* (2021) 1–767.
- [25] B. Bellalta, IEEE 802.11 ax: High-efficiency WLANs, *IEEE wireless communications* 23 (1) (2016) 38–46.
- [26] E. Khorov, A. Kiryanov, A. Lyakhov, G. Bianchi, A tutorial on IEEE 802.11 ax high efficiency WLANs, *IEEE Communications Surveys & Tutorials* 21 (1) (2018) 197–216.
- [27] E. J. Oughton, W. Lehr, K. Katsaros, I. Selinis, D. Bublely, J. Kusuma, Revisiting wireless internet connectivity: 5G vs Wi-Fi 6, *Telecommunications Policy* 45 (5) (2021) 102127.
- [28] A. Di Domenico, G. Perna, M. Trevisan, L. Vassio, D. Giordano, A network analysis on cloud gaming: Stadia, geforce now and psnow, *Network* 1 (3) (2021) 247–260.
- [29] M. Manzano, M. Uruena, M. Sužnjević, E. Calle, J. A. Hernandez, M. Matijasevic, Dissecting the protocol and network traffic of the OnLive cloud gaming platform, *Multimedia systems* 20 (5) (2014) 451–470.
- [30] M. Carrascosa, B. Bellalta, Cloud-gaming: Analysis of google stadia traffic, *Computer Communications* 188 (2022) 99–116.
- [31] S. Zhao, H. Abou-zeid, R. Atawia, Y. S. K. Manjunath, A. B. Sediq, X.-P. Zhang, Virtual reality gaming on the cloud: A reality check, in: 2021 IEEE Global Communications Conference (GLOBECOM), IEEE, 2021, pp. 1–6.
- [32] Y.-C. Li, C.-H. Hsu, Y.-C. Lin, C.-H. Hsu, Performance measurements on a cloud VR gaming platform, in: Proceedings of the 1st Workshop on Quality of Experience (QoE) in Visual Multimedia Applications, 2020, pp. 37–45.
- [33] E. Vikberg, et al., Optimizing WebRTC for Cloud Streaming of XR (2021).
- [34] G. Lee, W. J. Yun, Y. J. Ha, S. Jung, J. Kim, S. Hong, J. Kim, Y. K. Lee, Measurement Study of Real-Time Virtual Reality Contents Streaming over IEEE 802.11 ac Wireless Links, *Electronics* 10 (16) (2021) 1967.
- [35] E. Korneev, M. Liubogoshchev, E. Khorov, Studying Cloud-Based Virtual Reality Traffic, *Journal of Communications Technology and Electronics* 67 (12) (2022) 1500–1505.
- [36] S. Salehi, A. Alnajim, X. Zhu, M. Smith, C.-C. Shen, L. Cimini, Traffic characteristics of virtual reality over edge-enabled wi-fi networks, *arXiv preprint arXiv:2011.09035* (2020).
- [37] M. Lecci, M. Drago, A. Zanella, M. Zorzi, An open framework for analyzing and modeling XR network traffic, *IEEE Access* 9 (2021) 129782–129795.
- [38] F. Chiariotti, M. Drago, P. Testolina, M. Lecci, A. Zanella, M. Zorzi, Temporal Characterization and Prediction of VR Traffic: A Network Slicing Use Case, *IEEE Transactions on Mobile Computing* (2023).
- [39] A. ALHILAL, K. SHATILOV, G. TYSON, T. BRAUD, P. HUI, Network Traffic in the Metaverse: The Case of Social VR, in: 2023 IEEE 43rd International Conference on Distributed Computing Systems Workshops (ICDCSW), 2023.
- [40] M. Jansen, J. Donkervliet, A. Trivedi, A. Iosup, Can My WiFi Handle the Metaverse? A Performance Evaluation Of Meta’s Flagship Virtual Reality Hardware, in: Companion of the 2023 ACM/SPEC International Conference on Performance Engineering, 2023, pp. 297–303.
- [41] World Wide Web Consortium W3C, Identifiers for WebRTC’s Statistics API, <https://www.w3.org/TR/webrtc-stats/>, [Accessed: January 30, 2024] (August 2023).
- [42] M. Casasnovas, C. Michaelides, M. Carrascosa, B. Bellalta, VR



streaming over Wi-Fi using WebRTC, Zenodo, data set (2024).  
doi:10.5281/zenodo.10455828.

- [43] RFC 6184, RTP Payload Format for H.264 Video, <https://datatracker.ietf.org/doc/html/rfc6184>, [Accessed: January 30, 2024] (May 2011).
- [44] B. García, M. Gallego, F. Gortázar, A. Bertolino, Understanding and estimating quality of experience in WebRTC applications, *Computing* 101 (2019) 1585–1607.
- [45] Telecommunication Standardization Sector of ITU (ITU-T), Quality of service assurance-related requirements and framework for virtual reality delivery using mobile edge computing supported by imt-2020, ITU-T Recommendation Y.3109, International Telecommunication Union (ITU) (2021).  
URL <https://www.itu.int/rec/T-REC-Y.3109/en>
- [46] Telecommunication Standardization Sector of ITU (ITU-T), Functional requirements of E2E network platforms to enhance the delivery of cloud-VR services over integrated broadband cable networks, ITU-T Recommendation J.1631, International Telecommunication Union (ITU) (2021).  
URL <https://www.itu.int/rec/T-REC-J.1631/en>
- [47] RFC 7741, RTP Payload Format for VP8 Video, <https://datatracker.ietf.org/doc/html/rfc7741>, [Accessed: January 30, 2024] (March 2016).